European Journal of Mechanics / B Fluids 67 (2018) 79–86

Contents lists available at ScienceDirect

European Journal of Mechanics / B Fluids

journal homepage: www.elsevier.com/locate/ejmflu

Influences of upstream extensions on flow around a curved cylinder

Fengjian Jiang [a,*], Bjørnar Pettersen [a], Helge I. Andersson [b]

[a] Department of Marine Technology, Norwegian University of Science and Technology, NO-7491 Trondheim, Norway
[b] Department of Energy and Process Engineering, Norwegian University of Science and Technology, NO-7491 Trondheim, Norway

ARTICLE INFO

Article history:
Received 3 November 2016
Received in revised form 8 August 2017
Accepted 9 August 2017
Available online 14 August 2017

Keywords:
Curved cylinder
Boundary conditions
Wakes
Boundary layer

ABSTRACT

In simulations of flow around a concave curved cylinder, i.e. free-stream aligned with the plane of curvature and directed towards the inner face of the curvature, one cannot avoid interactions between the cylinder and the inlet boundary. To get rid of the effects brought about by this interaction, we consider different lengths of upstream straight extensions at the lower end of the curved cylinder (*0D*, *5D* and *10D*, where *D* is the cylinder diameter), referred to as horizontal extensions. In this study, we directly solve the time-dependent three-dimensional Navier–Stokes equations. Results reveal that the appended horizontal extension allows the boundary layer to develop, so that the velocity profile at the curved cylinder inception is significantly different from the case where no horizontal extension is considered. The laminar boundary layer is thinner than that in the flat plate flow, which is given by Blasius' solution. The results from *5D* and *10D* extensions show a clear convergent tendency. We therefore suggest that a horizontal extension is essential for concave curved cylinder flow simulation, and *10D* would be a preferred choice.

1. Introduction

We encounter a configuration of a curved cylinder in different marine engineering applications: for example, a flexible riser that connects the seabed and floating offshore structures, mooring lines, or pipelines to transport oil and gas. Due to its curved span, the wake behind a curved cylinder is considerably more complex than the wake of a straight cylinder, and becomes an interesting research topic. However, compared to the extensive studies on the straight cylinder wake, there are far less published results on a curved cylinder wake.

The curved cylinder is modeled as a quarter segment of a ring in most relevant studies; depending on the specific problem, straight extensions may be added to one or both ends of the quarter ring. Earlier studies of curved cylinders mostly focused on flow normal to the plane of curvature, as reviewed in previous publications [1,2]. Miliou et al. [3] first carried out fundamental studies of curved cylinder wakes with the inflow aligned with the plane of curvature. They studied flow past stationary curved cylinders at low Reynolds numbers of 100 and 500, and systematically reported the shedding pattern and wake topology. de Vecchi et al. [2] also studied the wake of curved cylinders at low Reynolds number $Re = 100$ and they considered both stationary cylinders and cylinders with forced cross-flow oscillations. Both studies observed distinctly different wake topologies when the inflow direction is reversed, i.e. bent vortex shedding when the inflow is towards the outer face of the curvature (referred to as *convex* configuration), but suppressed vortex shedding when the inflow is towards the inner face of the curvature (referred to as *concave* configuration). In addition, both studies attributed the suppression of vortex shedding in the concave configuration to an axial flow along the curvature, which makes the shear layer less susceptible to roll up and subsequently shed as a vortex street. Recently, Gallardo et al. [4] investigated the turbulent wake behind a convex curved cylinder at Reynolds number $Re = 3900$, in which they revealed distinct differences between the wake pattern in the upper part of the curved cylinder wake as compared to that in the lower part. Xu and Cater [5] reported a RANS study of a high Reynolds number flow ($Re = 1.5 \times 10^5$) around a curved cylinder, which was virtually a flexible riser model.

Unlike in simulations of flow past straight cylinders, where periodic boundary conditions are normally used at the two ends of the cylinders, special attention is essential for the boundary conditions at the two ends of the quarter ring. The above mentioned studies [1–4] all considered a straight extension normal to the free-stream direction (often referred to as a *vertical* extension) at one end of the quarter ring where a free-slip boundary condition was suggested. Gallardo et al. [6] carefully studied the free-slip boundary condition at this end of the quarter ring and the choice of a reasonable extension length.

* Corresponding author.
E-mail address: fengjian.jiang@ntnu.no (F. Jiang).

http://dx.doi.org/10.1016/j.euromechflu.2017.08.006
0997-7546/

Nomenclature

C_{Fi}	*Force coefficients* $C_{Fi} = F_i/0.5\rho U_0^2 S_p$
D	*Cylinder diameter*
f	*Frequency*
F_i	*Body forces* $F_i = (F_x, F_y, F_z)$
p	*Pressure*
Re	*Reynolds number* $Re = DU_0/\upsilon$
s	*Arc of cylinder centerline*
S	*Symmetric part of* $\nabla \boldsymbol{u}$
S_p	*Projection area of geometry*
St	*Strouhal number* $(St = fD/U_0)$
t	*Time*
$\boldsymbol{u} = (u, v, w)$	*Instantaneous velocity vector*
$\langle u\rangle, \langle v\rangle, \langle w\rangle$	*Time-averaged velocity*
U_0	*Inlet(freestream) velocity*
x, y, z	*Coordinates*
$\delta_{0.99}$	*Boundary layer thickness*
λ_2	*2nd largest eigenvalue of* $(S^2 + \Omega^2)$
$\nabla \boldsymbol{u}$	*Velocity gradient tensor*
Ω	*Antisymmetric part of* $\nabla \boldsymbol{u}$
ρ	*Density*
υ	*Kinematic fluid viscosity*

It is noteworthy that in the convex configuration, most previous studies [2–4] also considered another straight extension aligned with the free-stream direction at the other end of the quarter ring, which is often referred to as a *horizontal* extension. This horizontal extension continues all the way to the outlet of the flow domain. No free end will therefore appear in the cylinder wake. However, when it comes to the concave configuration, the horizontal extension was omitted in most numerical simulations [2,3]. To the authors' knowledge, the only study that considers a horizontal extension of a concave curved cylinder is an experimental investigation [1]. In that study the horizontal extension has a free end in the fluid and therefore induces additional disturbances to the incoming flow.

In the concave curved cylinder case reported by Miliou et al. [3], one end of the quarter ring interacts directly with the inlet surface. It is rather obvious that this direct interaction between the curved cylinder and inlet has some effects on the flow field. If one consider the most likely application of a curved cylinder, i.e. a deep-sea riser or a pipeline landing on the seabed, the curved part is most likely connected with straight extensions at both ends (horizontal and vertical). In this context, it is always difficult to isolate the curved part (quarter ring) from its straight extensions. Although Miliou et al. [3] gave a special treatment to the inflow boundary condition (as detailed in Section 2.1, viz Eq. (1)), the issue was left without any clarification.

In the present study, we aim to investigate the influence of a horizontal extension on the flow around a concave curved cylinder. Free ends in the computational domain are intentionally avoided to eliminate additional disturbances; so the horizontal extensions will start upstream and affect the inlet boundary conditions. Only one Reynolds number $Re = 100$ will be studied, while different lengths of the horizontal extension will be considered. This particular Re was chosen to enable direct comparisons with the results obtained by Miliou et al. [3]. Comparisons of the boundary layer flow along extensions of various lengths will be presented and the influence of the different extensions on the wake behind the curved part of the cylinder will be considered.

2. Numerical setups

2.1. Flow configuration

In this study, we consider a quarter ring curved circular cylinder, and a concave configuration is adopted, i.e. the free-stream

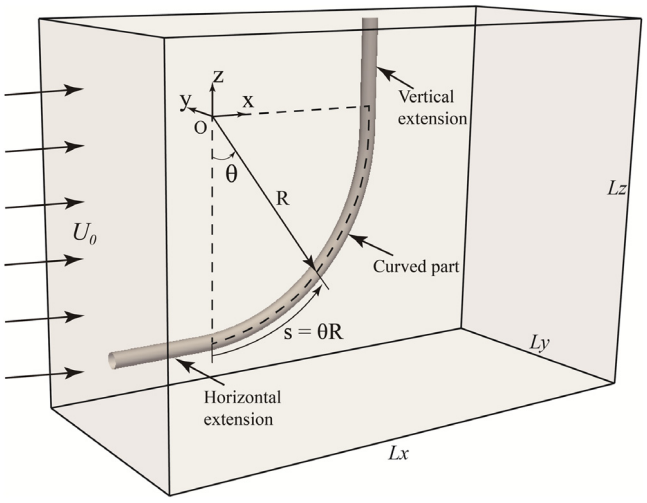

Fig. 1. Sketch of the geometry of the concave curved cylinder and the computational domain. The uniform inflow U_0 is from the left.

is directed towards the inner face of the ring. The geometry and the computational domain are depicted in Fig. 1. The radius of curvature is $R = 12.5D$, where R indicates the distance between the center of the ring (point O in Fig. 1) and the center of the circular cross sections, and D is the diameter of the circular cross-section. The Reynolds number is defined based on the free-stream velocity U_0 and D, i.e. $Re = U_0 D/\upsilon$, where υ is the kinematic fluid viscosity.

As shown in Fig. 1, the geometry studied here consists of three parts: a curved part (quarter ring), and two straight extensions at the two ends of it. We refer to them as the *vertical* (upper) extension and the *horizontal* (lower) extension, respectively. In order to study the effects caused by these straight extensions, we will consider some different combinations. An overview of the different cylinder configurations studied is given in Table 1.

As depicted in Fig. 1, we define the streamwise direction as the x-direction, the transverse direction as the y-direction, and the vertical direction as the z-direction, therefore the velocity vector writes $u_i = (u, v, w)$. For all cases, we adopted the same inflow boundary condition as that used by Miliou et al. [3]:

$$\frac{u}{U_0} = 1 - exp\left(-50\left(\sqrt{\left(\frac{y}{D}\right)^2 + \left(\frac{z}{D} + 12.5\right)^2} - 0.5\right)\right);$$
$$\frac{v}{U_0} = \frac{w}{U_0} = 0. \tag{1}$$

This velocity profile mimicks a very thin exponentially growing boundary layer profile at the intersection of the cylinder with the inlet computational boundary. The boundary layer profile defined by Eq. (1) will be shown later in Fig. 5. If we follow the most commonly used 0.99-criterion to define the boundary layer thickness $\delta_{0.99}$, Eq. (1) virtually represents a $\delta_{0.99} = 0.092D$ thick boundary layer, while further away from the cylinder geometry, the incoming free-stream remains uniform as U_0.

We imposed Neumann boundary conditions for the velocity components ($\partial u/\partial x = \partial v/\partial x = \partial w/\partial x = 0$) and zero pressure ($p = 0$) at the outlet of the flow domain. On the other four sides of the computational domain, we used free-slip boundaries, while the solid surface of the cylinder was treated as a no-slip boundary.

2.2. Numerical method

In this study, we directly solve the full Navier–Stokes equations:

$$\frac{\partial u_i}{\partial x_i} = 0 \tag{2}$$